Plant Physiol. (1997) 113: 111–118

Oscillations in H^+ and Ca^{2+} Ion Fluxes around the Elongation Region of Corn Roots and Effects of External pH[1]

Sergey Nikolayevich Shabala*, Ian Anstruther Newman, and John Morris[2]

Department of Physics, University of Tasmania, G.P.O. Box 252 C, Hobart, Tasmania 7001, Australia

Net fluxes of H^+ and Ca^{2+} around the elongation region of low-salt corn (*Zea mays* L.) roots were measured using the microelectrode ion flux estimation (MIFE) technique. At pH 5.2 two oscillatory components were found. Fast, 7-min oscillations in H^+ flux were superimposed on slow oscillations of about 1.5 h. Fast oscillations in Ca^{2+} flux showed a strong dependence on the H^+ oscillations and were normally leading in phase by about 1 to 1.5 min. Both oscillatory components were strongly affected by external pH values. Preincubation for 20 h in buffered pH 4.0 solution suppressed the slow oscillatory component and caused huge H^+ influxes in the elongation region. The fast oscillations were 8 times larger in amplitude and were slightly lengthened. Preincubation at pH 6.0 did not suppress the rhythmic character of the ion fluxes but it shifted the average H^+ flux to greater efflux. The fast and slow oscillatory components of H^+ flux seem to relate to biophysical and biochemical mechanisms of intracellular pH homeostasis, respectively. The origin of the Ca^{2+} flux oscillations is discussed in terms of the "weak acid Donnan Manning" model of cell wall ion exchanges.

Ion transport across cell membranes is controlled by a large number of positive and negative feedback systems (Felle, 1988a; Elzenga, 1989; Beffagna and Romani, 1991; Miedema and Prins, 1991). It is not surprising, therefore, that such systems exhibit oscillatory behavior. This appears in the regular fluctuations of membrane potential, ion permeability, and other bioelectrical characteristics (Berridge and Rapp, 1979). These oscillations are well documented, mainly in various fungal and algal cells (Gradmann and Slayman, 1975; Ogata and Kishimoto, 1976; Vucinic et al., 1978; Fisahn et al., 1986; Lucas and Fisahn, 1989). Experimental observations from higher plants are not as common.

However, as early as 1957 in this laboratory, Scott (1957) showed that bean roots possess a rhythmically changing electric field. Subsequent studies (Jenkinson and Scott, 1961; Jenkinson, 1962; Scott, 1962) demonstrated that both extracellular and intracellular root potentials exhibit 5-min oscillations, which appear spontaneously and can continue for 6 h. The amplitudes of those oscillations showed a strong dependence on bathing medium conditions (Jenkinson, 1962), whereas the periods were extremely stable. Similar conclusions were reached later (Souda et al., 1990; Toko et al., 1990) with regard to *Phaseolus* roots. The researchers also showed that the largest amplitudes of the bioelectric oscillations occur within the elongation region (Toko et al., 1990). The period of the oscillations was from 6 to 12 min and it varied with the elongation rate (Souda et al., 1990). A correlation between the amplitudes of bioelectric oscillations and the growth rate was also found for *Lepidium sativum* L. roots (Hecks et al., 1992), although they did not find a correlation between the growth rate and the frequency of the oscillations.

Microelectrode measurements on root cells (Jenkinson, 1962; Toko et al., 1990) did not provide an ionic basis for the oscillations observed. Too many possibilities for interpretation exist because many ions are involved in the generation of the cell membrane potential. In general, dynamic feedback control with oscillations provides an effective (Richter and Ross, 1980), accurate, stable, and noise-immune (Rapp et al., 1981) control mechanism for living cell homeostasis. Recent research has shown that ion distribution around plant roots is closely related to root development (Miller and Gow, 1989) and gravitropism (Zieschang et al., 1993), which indicates that modulation of ion redistribution might be one of the factors that modify root metabolism. For this reason the nature of the ionic basis of the bioelectric oscillations in roots must have great significance.

The introduction of the MIFE technique into the practice of physiological research (Lucas and Kochian, 1986; Newman et al., 1987) gives us the means to monitor ion dynamics around intact roots. In this study we report measurements of Ca^{2+} and H^+ fluxes around the elongation region of corn roots at various pH levels. Oscillations in ion fluxes are always detectable if the time of observation is long enough. Different oscillatory components of ion fluxes around plant roots seem to relate to different ion transport systems.

MATERIALS AND METHODS

Plant Material and Preparation

Corn seeds (*Zea mays* L., cv Aussie Gold) were surface-sterilized by immersion in 1% NaOCl for 10 min and then washed thoroughly in flowing, distilled water for 5 min.

[1] This work was supported by an Australian Research Council grant to I.A.N.

[2] Present address: Department of Electrical and Electronic Engineering, University of Western Australia, Nedlands, Western Australia 6907.

* Corresponding author; e-mail sergey.shabala@phys.utas.edu.au; fax 61–3–6226–2410.

Abbreviations: MIFE, microelectrode ion flux estimation; pH_o, external pH; VDI, valid data interval.

The seeds were spread on cotton gauze covering a plastic mesh suspended over aerated 0.2 mol m^{-3} $CaSO_4$ solution. The reasons for using low-salt roots have been discussed previously (Newman et al., 1987). Germination took place at 25°C in darkness. The seedlings were used for measurements on the 3rd d, when their root lengths were 60 to 80 mm. One-and-a-half hours before beginning measurements a seedling was taken from the incubation chamber and decapped to prevent gravitropic response. The root was placed in a Petri dish and the root cap was peeled gently from opposite sides of the tip and cut off with a scalpel blade. The decapped plant was placed immediately in a plexiglass measuring chamber that was 100 mm long, 30 mm deep, and 6 mm wide. Support for the root was provided by fine plexiglass partitions positioned 20 mm above the floor of the chamber and separated by about 40 mm. The root was centered within the chamber and fixed horizontally to these partitions with a cotton thread tied loosely at 7 and 40 mm from the root tip. The measuring chamber contained 12 to 15 mL of experimental bathing solution. Any refreshment of the solution was made at least 30 min before measurements to avoid transient changes in the ion fluxes due merely to solution change.

Solutions

We used 0.2 mol m^{-3} $CaSO_4$ (pH about 5.2) for pretreatment of seedlings and as the standard, unbuffered experimental solution. For experiments at a different pH this standard solution was replaced 20 h previously using a buffered solution of the desired pH. The buffered solutions were made with 2 mol m^{-3} Mes in 0.2 mol m^{-3} $CaSO_4$ and the pH was adjusted to the chosen value using 100 mol m^{-3} Tris buffer. Flux measurements were made in unbuffered solution for reasons given by Arif et al. (1995). Adjustments of pH in the unbuffered solution were made by the addition of 1% H_2SO_4 or 10 mol m^{-3} $Ca(OH)_2$.

Flux Measurements

Liquid-membrane, ion-selective microelectrodes pulled from borosilicate glass capillaries (GC150-10, Clark Electromedical Instruments, Pangbourne, UK) with tip diameters of about 2 μm were used in experiments. The electrode blanks were filled with commercially available cocktails (Fluka; H^+, 82500 and Ca^{2+} 21048). The back-filling solutions were 15 mol m^{-3} NaCl plus 40 mol m^{-3} KH_2PO_4 adjusted to pH 6.0 using NaOH for the H^+ microelectrode and 500 mol m^{-3} $CaCl_2$ for Ca^{2+}. The electrodes were calibrated in a known set of pH buffers (from 4.0 to 8.0) and standard Ca^{2+} solutions (from 0.05 to 1 mol m^{-3}) before and after use. The average responses of the electrodes were about 53 to 54 mV/pH for H^+ and 27 to 28 mV/pCa for Ca^{2+}. Electrodes with a response of less than 50 mV/pH or 25 mV/pCa were discarded. Resistance was about 2 GΩ. The reference electrode was a plastic tube containing 1000 mol m^{-3} KCl in 2% agar. The reference electrode was located in the solution at the end of the measuring chamber near the seed. The leakage of K^+ ions from the reference electrode was checked occasionally with K^+ ion-selective electrodes. The resulting concentration of K^+ ions in solution near the elongation region was less than 0.003 mol m^{-3}.

The ion-selective electrodes were mounted on a multimanipulator providing three-dimensional positioning. After the measuring chamber was placed in its holder the electrodes were positioned in a line parallel to the root axis 50 μm above the root surface. The distance between electrode tips was about 5 μm. During measurement the distance between the root surface and the electrodes was changed from 50 to 90 μm at a frequency of 0.1 Hz. This was achieved by fixing the holder with the measuring chamber on a three-way hydraulic micromanipulator (WR-88, Narishige, Tokyo, Japan) driven by a computer-controlled stepper motor (MO61-CE08, Superior Electric, Bristol, CT).

The new MIFE data recording system and flux calculation protocol have not, to our knowledge, previously been described. Signals from each electrode were digitized at a rate of about 20 samples per second using an analog-to-digital interface card installed in an IBM-compatible PC. The interface includes digital outputs. These outputs were used to control the stepper motor driving the micromanipulator and also to adjust the offset voltages of the custom-built, four-channel electrometer. Electrometer voltage offsets were necessary to permit a sensitivity of a few microvolts on a baseline of up to 300 mV. The interface was controlled by the software package CHART (Unitas Consulting, Hobart, Australia), which gave highest priority to secure transfer of the digitized data directly from the interface to a disc file. At a lower priority, CHART emulated the functions of a chart recorder by providing a real-time display on the screen (Fig. 1). After experiments were completed, the digitized data files could be re-displayed and converted by CHART to files containing simple columns of ASCII text. These files were used, together with the calibration data, to calculate mean net fluxes at 5-s intervals (each half-cycle of manipulator movement).

CHART has a provision for user-written routines to be added, which are invoked at the start, during, and the end of data acquisition runs. Routines were added that allowed

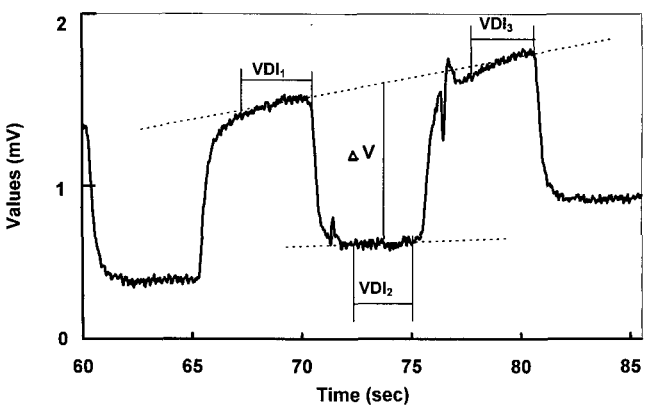

Figure 1. A typical segment of H^+ flux data recorded from one root to illustrate the method of calculating the voltage change from which the flux was calculated.

control of the offset voltages and the micromanipulator position automatically as well as in response to keyboard entries. Thus, the experiments were controlled interactively as data were acquired (inquiries about MIFE and CHART should be made to I.A.N. at the e-mail address: ian.newman@phys.utas.edu.au). These controlling changes were automatically incorporated into a log file, which was used subsequently by the flux calculation program. Another routine allowed comments to be inserted into the log file as the experiment progressed, facilitating analysis of the data when each acquisition run had been completed.

After the conclusion of the experiment the values of net fluxes across the tissue boundary were calculated from the recorded data, assuming cylindrical diffusion geometry outside the root (Newman et al., 1987; Kochian et al., 1992). The first stage in the calculation of ion flux was to calculate the mean voltage recorded at each extreme of manipulator movement. The first 1 or 2 s after the movement began were ignored to allow for both the movement (0.3 s) and the electrochemical settling of the electrodes.

The procedure is illustrated in Figure 1. At 60 s the manipulator moved the electrodes to the position close (20 μm) to the tissue surface. The electrochemical potential measured by the electrode quickly decreased by about 1 mV equivalent (with an origin that is dependent on the existing solution pH and the electrometer offset). At 65 s the manipulator moved the electrodes to the more distant (60 μm) position and the electrochemical potential increased again. The cycle was repeated with the 10-s period. The higher electrochemical potential at the more distant position means a higher concentration at that position for the H^+ (positive) ion in this example. The associated diffusive movement of the ion down its electrochemical potential gradient is toward the tissue, i.e. there is a net influx. To calculate the magnitude of this net influx, the electrometer's ΔV (the electrical voltage equivalent of the electrochemical potential difference over the distance Δx moved by the electrode tip) was found as follows.

A valid data interval was defined as the time interval (3 s in Fig. 1) for which the measured voltage had become settled, after the electrode movement and up to the start of the following movement. Three consecutive VDIs (VDI_1, VDI_2, and VDI_3 in Fig. 1) were chosen and the mean values of the mV data points for each were calculated. A line was drawn between the mean mV values for VDI_1 and VDI_3. The ΔV used in the flux calculation was the vertical distance from the mean mV value for VDI_2 to this line, as shown in Figure 1. The flux value was regarded as being at the midtime of VDI_2. For the flux 5 s later, VDI_1 was dropped and the next VDI was added to create the next triplet, which would be treated similarly. Fluxes were calculated by this process at 5-s intervals and are thus effectively running averages over 10 to 15 s.

The above procedure makes reasonable allowance for the settling time of the electrochemical potential at the electrode tip after the electrode movement. It also allows for drift of the signal, as seen in Figure 1, which is to be expected when the tissue flux causes changes in the concentration of the ion being measured. Ion concentrations close to the root were calculated from the calibration data and from the average mV value for the two positions. Hence, the pH values reported are at about 70 μm from the root.

Statistics

Up to 10 different plants were measured for 2 h in each variant. Because of the wide spectrum and different phases of rhythmic activity, direct averaging of ion fluxes from individual plants produced a loss of valuable information. For example, if 2 different plants show the same oscillatory component but 1 is shifted by about one-half of the period of the component, such oscillations cancel each other out during averaging. Consequently, we present representative temporal curves for each variant (Fig. 2). For the main descriptive parameters, means, SES, and sample sizes are tabulated. For each fast-oscillation half-cycle, its amplitude was measured as the difference between the peak and the trough fluxes. The average amplitude of the fast-ion oscillations was calculated as the mean of those differences for all oscillatory cycles having amplitudes more than 5 nmol m^{-2} s^{-1}, which was about the order of the noise during measurements. To calculate the mean maximum amplitude of the fast-ion oscillations, the values of the three largest half-cycle amplitudes were taken for each of 6 to 8 individual plants. Phase shift between the fast Ca^{2+} and H^+ oscillations was calculated as the average time interval between the times when Ca^{2+} and H^+ fluxes reached their minimum values during the fast oscillatory cycles.

RESULTS

In spite of some variability in the quantitative characteristics, all plants showed similar changes with time in net H^+ and Ca^{2+} fluxes. Typical Ca^{2+} and H^+ fluxes for each variant are shown in Figure 2. The common features of the ion fluxes are described in Table I, and the quantitative information is given in Table II. Qualitatively similar oscillations have been observed from roots at times up to 5 h at least after decapping (data not shown). Thus, the injury due to decapping does not determine the oscillations.

Figure 2A shows typical Ca^{2+} and H^+ fluxes around the elongation region in the control (unbuffered 0.2 mol m^{-3} $CaSO_4$, pH 5.2). Both fluxes were extremely variable during 2 h of continuous measurements. H^+ fluxes showed at least two major oscillatory components: slow, rhythmic changes with periods of about 1.5 h and fast oscillations with periods of about 7 min. The slow H^+ changes usually started as net efflux, changed in 30 to 40 min to influx, and then changed back again. The average value of the H^+ flux during the 2 h was negative (net efflux), which caused the pH around the measured site to be about 4.8 instead of 5.2, as for the bulk solution. Local pH is a useful representation of the sum (integral) of the H^+ fluxes up to that time. The pH is also affected by H^+ fluxes at more distant regions. Slow, rhythmic changes of proton flux were always accompanied by slow, local pH changes with the same period.

The fast H^+ flux oscillations appeared reliably at a similar phase of the slow H^+ changes. The amplitudes of the

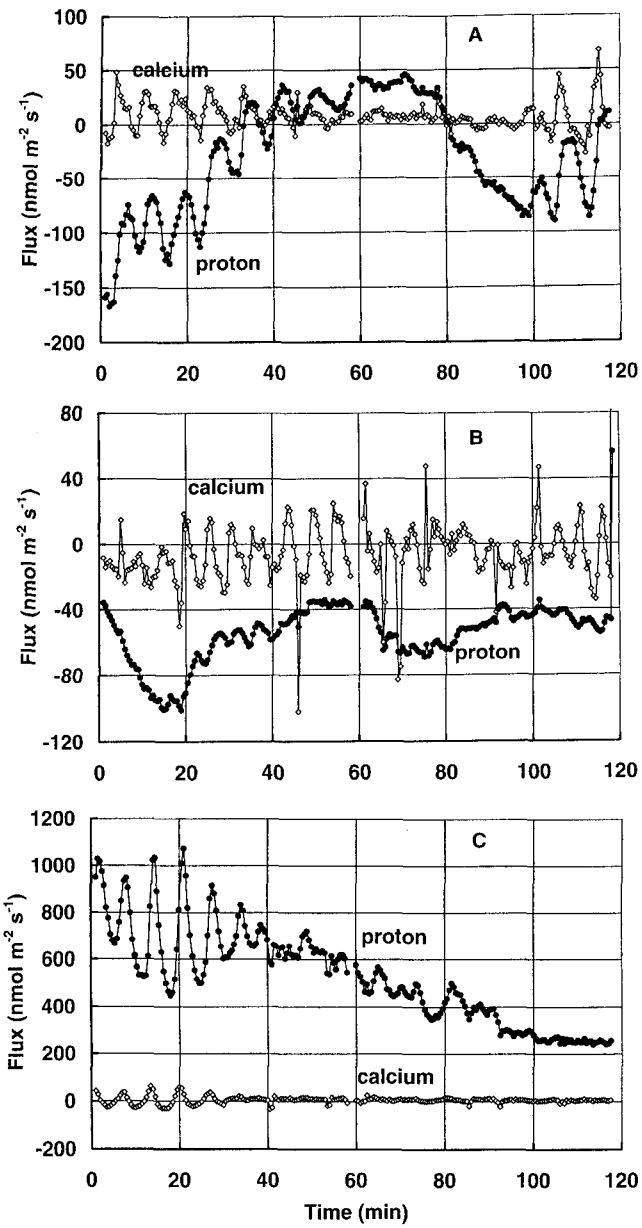

Figure 2. H^+ (closed symbols) and Ca^{2+} (open symbols) net fluxes (inward positive) around the elongation region of corn roots. Representative records from one individual plant in each variant are shown. A, Control, pH 5.2; B, pH 6.0; C, pH 4.0. Measurements were made at 5-s intervals. Each point represents the average value of the six measurements during 30 s. Fast and slow oscillatory components are clearly seen in controls, and at pH 6.0. Slow oscillations are suppressed at pH 4.0.

fast oscillations were extremely variable and changed from a maximum of about 100 nmol m^{-2} s^{-1} to 0 and back again. They appeared predominantly on the ascending part of the slow H^+ curve, and their amplitude showed a strong dependence on the gradient and direction of the pH changes during the slow H^+ flux cycle (Fig. 3).

Ca^{2+} fluxes also showed two oscillatory components. Unlike the H^+ oscillations, the fast, 7-min oscillatory component of Ca^{2+} flux always occurred around a small but steady net influx. The slow component of the Ca^{2+} fluxes appeared instead as a factor modulating the amplitude of the fast, 7-min oscillations. In phase, the fast Ca^{2+} oscillations always led the fast proton oscillations by about 1.5 min, and there was a close relationship between their amplitudes (Fig. 4).

Pretreatment for 20 h in a buffered solution of pH 6.0 did not eliminate the rhythmic character of ion fluxes (Fig. 2B) and both slow and fast oscillatory components appeared when measured at pH 6.0. The amplitudes and periods of both slow and fast H^+ flux oscillations were reduced (Table II). The average proton flux was more negative, and the slow, rhythmic H^+ changes always occurred in the negative region, indicating a continuous net efflux without transition through the zero line, as in the control (Fig. 2A). The average Ca^{2+} flux also became negative and the period of the fast Ca^{2+} oscillations was reduced in the same way as for H^+. However, the amplitude characteristics of the Ca^{2+} oscillations remained as for the control.

Acidification of the bulk solution (plant pretreatment with buffered pH 4.0 and measurement in unbuffered pH 4.0 $CaSO_4$) produced dramatic changes in the flux behavior (Fig. 2C). Net H^+ fluxes were always positive (influx). They started with very large values of about 800 nmol m^{-2} s^{-1} and tended to reduce in a linear way during 2 h of measurements. The average value was about 500 nmol m^{-2} s^{-1}. Fast proton oscillations were found for 40% of measured plants. They also had very large amplitude: up to 560 nmol m^{-2} s^{-1} (Table II), which was 5 times larger than the control. The average Ca^{2+} fluxes were slightly positive and showed fast oscillations when H^+ oscillations were present. Average Ca^{2+} amplitudes were about 1.5 times larger than the control. We also observed that the fast oscillatory component for both H^+ and Ca^{2+} fluxes slowed in the acid solution (Table II).

DISCUSSION

Effect of External pH on H^+ Flux

Cytosolic pH has been found to regulate key metabolic processes in plant tissues (Felle, 1988a; Sanders and Slayman, 1989; Beffagna and Romani, 1991). Because cytoplasmic pH is about 7.0 for most plants (Smith and Raven, 1979; Felle, 1988a), and because of the negative plasma membrane potential, H^+ influx is energetically favorable. However, in this study we found that there was strong acidification of external solution around the elongation region (pH_o 4.8 instead of the bulk solution 5.2). This is in agreement with other reports (Pilet et al., 1983; Zieschang et al., 1993) and requires the active extrusion of H^+ via H^+-ATPases, which also generates the large negative membrane potential. Both passive and active H^+ transport systems seem to be sensitive to external pH_o changes. There is some evidence that pH_o acts mainly on passive membrane characteristics and modifies H^+-channel conductivity (Spanswick, 1981; Smith and Walker, 1985; Elzenga, 1989). However, H^+-channels are still very poorly documented (Felle, 1988a) and these conclusions need to be confirmed

Table I. *Qualitative characteristics of ion fluxes around the elongation region of corn roots*

Parameter	pH 4.0	pH 5.2 (Control)	pH 6.0
Long-term H^+ flux features	Near-linear decrease with time, starting as huge influx and remaining positive	Oscillatory, usually starting as efflux, changing to influx and back again	Oscillatory, remaining negative
Long-term Ca^{2+} flux features	Steady average value	Steady average value	Steady average value
Existence of fast H^+ oscillations	Present in about 40% of cases	Present in every measurement	Present in every measurement
Typical traits of fast H^+ oscillations	Amplitude unrelated to slow H^+ changes	Amplitude depends strongly on phase of slow H^+ changes	Amplitude depends strongly on phase of slow H^+ changes
Existence of fast Ca^{2+} oscillations	Present when H^+ oscillations are present	Present in every measurement	Present in every measurement
Typical traits of fast Ca^{2+} oscillations	Amplitude is related to fast H^+ amplitude	Amplitude is modulated by slow H^+ changes	Amplitude is modulated by slow H^+ changes

in future experiments. Other arguments support H^+-ATPases as the main H^+-transport systems sensitive to pH_o (Kawamura et al., 1980; Reid et al., 1985).

More interesting is the effect of pH_o on the oscillatory behavior of H^+ fluxes. Our results show the existence of at least two oscillatory components of H^+ flux. One is slow, with a period of about 1.5 h, and the other is fast, with a period of about 7 min. Such a difference in periods suggests that it is unlikely that only one ion transport system is involved.

We propose that the slow, rhythmic changes of H^+ fluxes around the elongation region are due to oscillations in behavior of passive H^+ transporters and that the fast, 7-min oscillations are due to oscillations in electrogenic H^+-ATPases. We support these proposals with the following arguments. Long-term regulation of intracellular pH includes both biophysical and biochemical mechanisms (Smith and Raven, 1979; Felle, 1988a). Biophysical pH regulation is achieved via a feedback relation, including cytosolic pH and plasma membrane potential (Beffagna and

Table II. *Quantitative characteristics of ion fluxes and pH around the elongation region of corn roots*

Probabilities compared with control by Student's *t* test. Results are means ± SE (*n* = sample size).

Parameters	pH 4.0	pH 5.2 (Control)	pH 6.0
Average value of H^+ flux during 2 h, nmol m^{-2} s^{-1}	520 ± 53[a] (*n* = 12)	−24.9 ± 3.6 (*n* = 16)	−56.1 ± 9.6[b] (*n* = 14)
Average value of Ca^{2+} flux during 2 h, nmol m^{-2} s^{-1}	6.49 ± 1.31 (*n* = 12)	4.61 ± 1.28 (*n* = 16)	−0.21 ± 1.38[c] (*n* = 14)
Average value of pH during 2 h, pH units	4.06 ± 0.036[a] (*n* = 12)	4.81 ± 0.016 (*n* = 16)	5.20 ± 0.03 (*n* = 14)[a]
Half-period of slow H^+ oscillations, min	None	44.5 ± 5.25 (*n* = 7)	29.7 ± 1.9[c] (*n* = 13)
Half-period of slow pH oscillations, min	None	45.33 ± 5.33 (*n* = 12)	30.7 ± 1.62[c] (*n* = 9)
Average amplitude of slow H^+ oscillations, nmol m^{-2} s^{-1}	None	131.2 ± 20.4 (*n* = 16)	47.0 ± 4.53[b] (*n* = 13)
Average amplitude of slow pH oscillations, pH units	None	0.12 ± 0.019 (*n* = 6)	0.067 ± 0.006[c] (*n* = 12)
Maximum changes in H^+ flux during 2 h, nmol	583 ± 65[b] (*n* = 6)	173 ± 30 (*n* = 8)	76.8 ± 8.8[c] (*n* = 6)
Maximum changes in pH during 2 h, pH units	0.16 ± 0.03[b] (*n* = 6)	0.18 ± 0.03 (*n* = 7)	0.15 ± 0.029 (*n* = 6)
Period of fast H^+ oscillations, min	7.84 ± 0.21[b] (*n* = 22)	7.01 ± 0.12 (*n* = 69)	6.40 ± 0.15[b] (*n* = 75)
Period of fast Ca^{2+} oscillations, min	7.77 ± 0.23[c] (*n* = 18)	7.18 ± 0.10 (*n* = 75)	6.24 ± 0.11[a] (*n* = 93)
Average amplitude of fast H^+ oscillations, nmol m^{-2} s^{-1}	359 ± 27[a] (*n* = 39)	48.2 ± 3.02 (*n* = 138)	25.6 ± 1.94[a] (*n* = 161)
Average amplitude of fast Ca^{2+} oscillations, nmol m^{-2} s^{-1}	63.2 ± 5.05[a] (*n* = 37)	43.4 ± 1.79 (*n* = 134)	44.8 ± 1.60 (*n* = 188)
Maximum amplitude of fast H^+ oscillations, nmol m^{-2} s^{-1}	560 ± 41[a] (*n* = 9)	103.2 ± 11.7 (*n* = 18)	52.5 ± 8.46[b] (*n* = 21)
Maximum amplitude of fast Ca^{2+} oscillations, nmol m^{-2} s^{-1}	96.6 ± 9.07[c] (*n* = 9)	70.9 ± 4.09 (*n* = 18)	72.4 ± 6.34 (*n* = 21)
Phase shift between fast Ca^{2+} and H^+ oscillations, min	0.84 ± 0.07[b] (*n* = 21)	1.45 ± 0.17 (*n* = 69)	1.30 ± 0.098 (*n* = 85)

[a] $P < 0.001$. [b] $P < 0.01$. [c] $P < 0.05$.

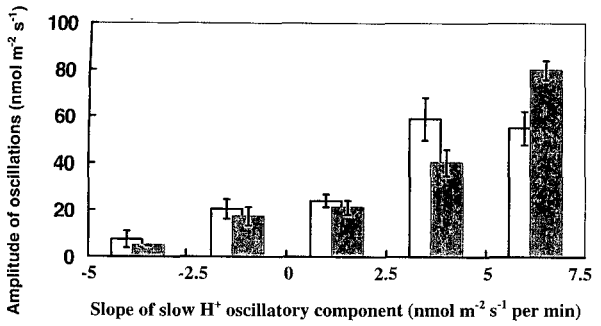

Figure 3. Amplitude of fast Ca^{2+} (open) and H^+ (shaded) flux oscillations at pH 5.2 as a function of the magnitude and direction of the slow H^+ flux oscillatory component. The amplitudes of ion flux oscillations were greatest for the largest slope of slow H^+ flux oscillations. The slope of the slow H^+ flux oscillatory component was calculated every 20 min for 2 h of measurement for each plant, and amplitudes of ion flux oscillations were plotted against the calculated slope. Error bars are SES; total sample size $n = 78$.

Romani, 1991). This is a relatively fast mechanism, operating within minutes (Roberts et al., 1981; Felle, 1988b). The biochemical pH-stat functions mainly via natural buffers (bicarbonate, phosphate compounds, and amino acids) operating at approximately pH 6.0 to 8.0 (Smith and Raven, 1979). All of these metabolic events have large temporal constants and produce a slow regulatory chain in plant cells. Hence, the fast and slow oscillatory components in H^+ fluxes around the elongation region of corn roots may be related to the fast and slow pH-stat mechanisms in plant cells.

Fast oscillations of H^+ fluxes in roots at pH 5.2 showed a strong relationship with the direction and gradients of the slow H^+ flux changes (and hence pH_o) caused by the long-period oscillatory component (Fig. 3). Their amplitude was largest when the slope of the slow H^+ oscillatory component was largest and positive, i.e. when the cytosol was being made less alkaline most rapidly by the H^+ flux. Thus, our argument that the fast, 7-min component is caused by H^+-pump oscillatory behavior is in accord with effects of IAA (Felle, 1988b), fusicoccin (Roberts et al., 1981), and organic weak acid (Beffagna and Romani, 1991), all of which stimulate the electrogenic H^+ pump by acidifying the cytosol.

After 20 h of pretreatment in buffered pH 4.0 solution the large chemical $[H^+]$ gradients between the cytosol and the bulk solution caused the observed large H^+ influx through unspecified transporters. The resulting continued acidification of the cytosol would compel particularly active H^+ extrusion via H^+-pumps. In this case the fast oscillations were 8 times larger in amplitude than for the control (Table II). The slow oscillatory component of H^+ flux was suppressed. One possibility is that all available intracellular buffers were exhausted after long-term preincubation. Consequently, the biochemical pH-stat was saturated and "switched off," removing the slow, rhythmic variations and leaving only the fast component (Fig. 2C).

External solution at pH 6.0 reduced the H^+ electrochemical gradient between the cytosol and the external solution. As a result, the H^+ influx was weakened and the net proton flux was more negative than for the control. Since pH_o 6.0 is not far from the normal physiological range, a neutral cytosol was easily maintained with both mechanisms active. Because the biochemical pH-stat was active, the slow oscillatory component was present (Fig. 2B) and with smaller amplitude (Table II). Fast oscillations also occurred but with about one-half of the control amplitude (Table II), indicating lower activity of the extrusion pump.

Thus, it is likely that fast and slow oscillatory components of H^+ fluxes around corn roots are related to the biophysical and biochemical mechanisms of intracellular pH homeostasis, respectively. The first is supposed to be mainly via electrogenic H^+-extrusion; the second may be related to the changes in passive membrane conductivity to H^+. One way to confirm this distinction is with long-term (at least 1.5 h) measurements of membrane resistance. No previous microelectrode studies extended beyond 10 min (Felle, 1988a), so they are not useful in solving the problem. The situation is complicated by the need to move measuring electrodes as the root grows.

Effect of External pH on Ca^{2+} Flux

Ca^{2+} also plays a key role in plant growth and development, regulating a variety of cellular processes ranging from the control of ion transport to gene expression (Bush, 1995). Its role as a second messenger is widely supported (Felle, 1988a, 1988b; Schroeder and Thuleau, 1991; Bush, 1995). Ca^{2+} transport across these membranes may occur via various mechanisms. These may include voltage-dependent (Bush, 1995), ABA-activated (Schroeder and Hagiwara, 1990), and stretch-activated (Pickard and Ding, 1993) Ca^{2+} channels, active transport using Ca^{2+}-ATPases (Bush, 1995), and a Ca^{2+}/nH^+ antiport system (Blackford et al., 1990). All of them are potential sources of our observed Ca^{2+} flux oscillations.

Oscillations in cytosolic-free Ca^{2+} have been reported after auxin (Felle, 1988b), ABA (Schroeder and Hagiwara, 1990), or Ca^{2+} treatment (McAinsh et al., 1995), all with periods within the 5- to 20-min range. The oscillatory mechanism is still unknown; however, there is some evi-

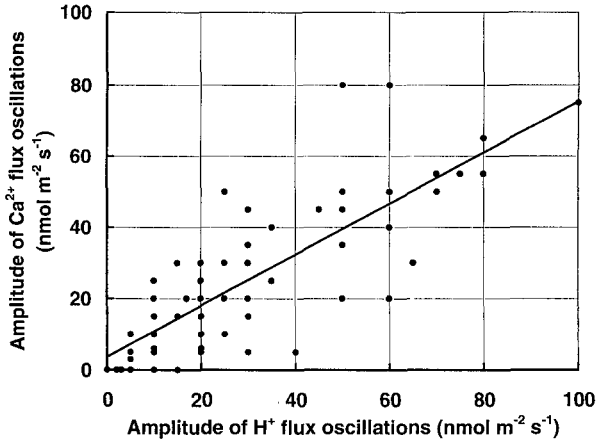

Figure 4. Association between the amplitude of Ca^{2+} and H^+ flux oscillations at pH 5.2. A least squares line of best fit is shown ($n = 78$).

dence that information about external factors affecting the cell may be encoded in the magnitude of the Ca^{2+} changes and in the temporal characteristics of the oscillations (Bush, 1995; McAinsh et al., 1995). Therefore, this oscillatory encoding may be of great significance in the cell-environmental interaction.

There is another source of oscillations in Ca^{2+} flux as measured around the corn roots. This is the Ca^{2+} residing in and released from the cell walls after exchange with H^+. Richter and Dainty (1989, 1990) developed the "weak acid Donnan Manning" model, which can be used to describe quantitatively the ion-exchange properties of a cell wall. This model has been developed further in our laboratory (Ryan et al., 1992; Arif and Newman, 1993) and shows that oscillating H^+ fluxes cause oscillatory Ca^{2+} fluxes around the root.

Our results show a strong correlation between fast oscillations in Ca^{2+} and H^+ fluxes. As the amplitude of H^+ oscillations increased so did the Ca^2 amplitude (Fig. 4). Ca^{2+} oscillations were always leading (Table II), with a phase shift of about 1 to 1.5 min. The slow oscillatory component of H^+ fluxes modulated the amplitude values of fast Ca^{2+} oscillations (Fig. 2A). Both of these features are in agreement with the weak acid Donnan Manning model. Arif and Newman (1993) showed that initial H^+ extrusion into the wall displaces Ca^{2+}, which will emerge into the external solution before the external H^+ flux is seen. Thus, our observations support the existence of a secondary source of Ca^{2+} oscillations, the cell walls, and the existence of a Ca^{2+} release mechanism from cell walls. Do these Ca^{2+} oscillations occur solely as the result of the exchange with other ions (H^+ in this study) as proposed by Ryan et al. (1992), or are they part of a general oscillatory mechanism that also includes membrane oscillators?

It seems likely that both membrane and wall Ca^{2+} are involved. If Ca^{2+} from the cell wall is the sole source of the Ca^{2+} flux around corn root, we expect pH changes to have a similar effect on the amplitude characteristics of the flux oscillations of both Ca^{2+} and protons. However, the use of acid medium did not affect the average Ca^{2+} flux during 2 h of measurements. Whereas the amplitude of the fast H^+ oscillations was 8 times the control amplitude, the Ca^{2+} amplitude was only 1.5 times greater (Table II). Again, when amplitudes of the H^+ flux oscillations were reduced by a factor of 2 following pH 6.0 treatment (Table II), the Ca^{2+} oscillation amplitude remained unchanged. Although detailed modeling of wall H^+/Ca^{2+} exchange has not been done, these arguments support the existence of cytosol/membrane Ca^{2+} oscillators as well as wall exchange. It is still unclear whether changes in cytosolic pH normally drive changes in cytosolic-free Ca^{2+} or vice versa (Bush, 1995). Nevertheless, the interdependence of H^+ and Ca^{2+} regulation is important in plant cells (Felle, 1988b) and is one of the possible mechanisms for the synchronization of Ca^{2+} and H^+ oscillations.

ACKNOWLEDGMENT

The authors are grateful to Mr. A. Knowles for technical assistance in the preparation of this manuscript.

Received June 3, 1996; accepted September 22, 1996.

LITERATURE CITED

Arif I, Newman IA (1993) Proton efflux from oat coleoptile cells and exchange with wall calcium after IAA or fusicoccin treatment. Planta **189:** 377–383

Arif I, Newman IA, Keenlyside N (1995) Proton flux measurements from tissues in buffered solution. Plant Cell Environ **18:** 1319–1324

Beffagna N, Romani G (1991) Modulation of the plasmalemma proton pump activity by intracellular pH in *Elodea densa* leaves: correlation between acid load and H^+ pumping activity. Plant Physiol Biochem **29:** 471–480

Berridge MJ, Rapp PE (1979) A comparative survey of the function, mechanism and control of cellular oscillators. J Exp Biol **81:** 217–279

Blackford S, Rea PA, Sanders D (1990) Voltage sensitivity of H^+/Ca^{2+} antiport in higher plant tonoplast suggest a role in vacuolar calcium accumulation. J Biol Chem **265:** 9617–9620

Bush DS (1995) Calcium regulation in plant cells and its role in signaling. Annu Rev Plant Physiol Plant Mol Biol **46:** 95–122

Elzenga JTM (1989) Mechanism for bicarbonate utilization in water plants. PhD thesis. University of Groningen, The Netherlands

Felle H (1988a) Short-term pH regulation in plants. Physiol Plant **74:** 583–591

Felle H (1988b) Auxin causes oscillations of cytosolic free calcium and pH in *Zea mays* coleoptiles. Planta **174:** 495–499

Fisahn J, Mikschl E, Hansen U-P (1986) Separate oscillations of the electrogenic pump and of a K^+-channel in *Nitella* as revealed by simultaneous measurement of membrane potentials and resistance. J Exp Bot **37:** 34–47

Gradmann D, Slaymann CL (1975) Oscillations of an electrogenic pump in the plasma membrane of *Neurospora.* J Membr Biol **23:** 181–212

Hecks B, Hejnowicz Z, Sievers A (1992) Spontaneous oscillations of extracellular electrical potentials measured on *Lepidium sativum* L. roots. Plant Cell Environ **15:** 115–121

Jenkinson IS (1962) Bioelectric oscillations of bean roots: further evidence for a feedback oscillator. II. Intracellular plant root potentials. Aust J Biol Sci **15:** 101–114

Jenkinson IS, Scott BIH (1961) Bioelectric oscillations of bean roots: further evidence for a feedback oscillator. I. Extracellular response to oscillations in osmotic pressure and auxin. Aust J Biol Sci **14:** 231–236

Kawamura G, Shimmen T, Tazawa M (1980) Dependence of the membrane potential of *Chara* cells on external pH in the presence or absence of internal adenosinetriphosphate. Planta **149:** 213–218

Kochian LV, Shaff JE, Kuhtreiber WM, Jaffe LF, Lucas WJ (1992) Use of extracellular, ion selective, vibrating microelectrode system for the quantification of K^+, H^+, and Ca^{2+} fluxes in maize roots and maize suspension cells. Planta **188:** 601–610

Lucas WJ, Fisahn J (1989) Oscillations and inversion in the extracellular current profiles of *Chara* and *Nitella. In* J Dainty, MI De Michelis, E Marre, F Rasi-Caldogno, eds, Plant Membrane Transport: The Current Position. Elsevier, New York, pp 25–29

Lucas WJ, Kochian LV (1986) Ion transport processes in corn roots: an approach utilizing microelectrode techniques. *In* WD Gensler. ed, Advanced Agricultural Instrumentation, Design and Use. Martinus Nijhoff, Dordrecht, The Netherlands, p 402

McAinsh MR, Webb AAR, Taylor JE, Hetherington AM (1995) Stimulus-induced oscillations in guard cell cytosolic free calcium. Plant Cell **7:** 1207–1219

Miedema H, Prins HBA (1991) pH-dependent proton permeability of the plasma membrane is a regulating mechanism of polar transport through the submerged leaves of *Potamogeton lucens.* Can J Bot **69:** 1116–1122

Miller AL, Gow NAR (1989) Correlation between profile of ion-current circulation and root development. Physiol Plant **75:** 102–108

Newman IA, Kochian LV, Grusak MA, Lucas WJ (1987) Fluxes of H^+ and K^+ in corn roots. Plant Physiol **84:** 1177–1184

Ogata K, Kishimoto U (1976) Rhythmic change of membrane potential and cyclosis of *Nitella* internode. Plant Cell Physiol **17:** 201–207

Pickard BG, Ding JP (1993) The mechanosensory calcium-selective ion channel: key component of a plasmalemma control centre? Aust J Plant Physiol **20:** 439–459

Pilet P-E, Versel JM, Mayor G (1983) Growth distribution and surface pH pattern along maize roots. Planta **158:** 398–402

Rapp PE, Mees AI, Sparrow CT (1981) Frequency encoded biochemical regulation is more accurate than amplitude dependent control. J Theor Biol **90:** 531–544

Reid RJ, Dejaegere R, Pitman MG (1985) Regulation of electrogenic pumping in barley by pH and ATP. J Exp Bot **36:** 535–549

Richter C, Dainty J (1989) Ion behaviour in plant cell walls. I. Characterization of the *Sphangum russowii* cell wall ion exchanger. Can J Bot **67:** 451–459

Richter C, Dainty J (1990) Ion behaviour in plant cell walls. IV. Selective cation binding by *Sphangum russowii* cell walls. Can J Bot **68:** 773–781

Richter PH, Ross J (1980) Oscillations and efficiency in glycolysis. Biophys Chem **12:** 285–297

Roberts JKM, Ray PM, Wade-Jardetzky N, Jardetzky O (1981) Extent of intracellular pH changes during H^+ extrusion by maize root-tip cells. Planta **152:** 74–78

Ryan PR, Newman IA, Arif I (1992) Rapid calcium exchange for protons and potassium in cell walls of *Chara*. Plant Cell Environ **15:** 675–683

Sanders D, Slayman CL (1989) Transport at the plasma membrane of plant cells: a review. *In* J Dainty, MI DeMichelis, E Marré, F Rasi-Caldogno, eds, Plant Membrane Transport: The Current Position. Elsevier, New York, pp 3–11

Schroeder JL, Hagiwara S (1990) Repetitive increases in cytosolic Ca^{2+} of guard cells by abscisic acid activation of nonselective Ca^{2+}-permeable channels. Proc Natl Acad Sci USA **87:** 9305–9309

Schroeder JI, Thuleau P (1991) Ca^{2+} channels in higher plant cells. Plant Cell **3:** 555–559

Scott BIH (1957) Electrical oscillations generated by plant roots and a possible feedback mechanism responsible for them. Aust J Biol Sci **10:** 164–179

Scott BIH (1962) Feedback-induced oscillations of five-minute period in the electric field of the bean root. Annu New York Acad Sci **98:** 890–900

Smith FA, Raven JA (1979) Intracellular pH and its regulation. Annu Rev Plant Physiol **30:** 289–311

Smith JR, Walker NA (1985) Effects of pH and light on the membrane conductance measured in the acid and basic zones of *Chara*. J Membr Biol **83:** 193–205

Souda M, Toko K, Hayashi K, Fujiyoshi T, Ezaki S, Yamafuji K (1990) Relationship between growth and electric oscillations in bean roots. Plant Physiol **93:** 532–536

Spanswick RM (1981) Electrogenic ion pumps. Annu Rev Plant Physiol **32:** 267–289

Toko K, Souda M, Matsuno T, Yamafuji K (1990) Oscillations of electrical potential along a root of a higher plant. Biophys J **57:** 269–279

Vucinic Z, Radenovic C, Damjanovic Z (1978) Oscillations of the vacuolar potential in *Nitella*. Physiol Plant **44:** 181–186

Zieschang HE, Kohler K, Sievers A (1993) Changing proton concentrations at the surfaces of gravistimulated *Phleum* roots. Planta **190:** 546–554